American Journal of Nanotechnology & Nanomedicine

Research Article

Atorvastatin in PLGA-PEG Nanoparticles Derivatized with the HIV-TAT Peptide Protects Neuronal Cultures in an Oxygen-Glucose Deprivation (OGD) Model -

Angel Cespedes[1,4], Maria Jose Perez[2,4], Maria Jose Gomara[3], Francisco Wandosell[4,5]*, Isabel Haro[3]

[1]*Research Group of Neurodegenerative Diseases, Department of Animal Health, Faculty of Veterinary Medicine and Zootechnics-Tolima University, Santa Helena-730006299, Ibagué-Colombia*

[2]*Department of Biology (Animal Physiology)-Faculty of Sciences - Universidad Autónoma de Madrid. C/Darwin 2. 28049 Madrid-Spain*

[3]*Unit of Synthesis and Biomedical Applications of Peptides, Department of Biological Chemistry, IQAC-CSIC, Jordi Girona 18, 08034 Barcelona, Spain*

[4]*Molecular Biology Center "Severo Ochoa", Department of Molecular Neuropathology CSIC-UAM. Nicolás Cabrera 1, 28049 Madrid-Spain*

[5]*Network Biomedical Research Center on Neurodegenerative Diseases (CIBERNED), Spain*

***Address for Correspondence:** Francisco Wandosell, Department of Molecular Neuropathology CSIC-UAM & CIBERNED. Nicol s Cabrera 1, 28049 Madrid-Spain, Tel: +349-119-645-61; E-mail: fwandosell@cbm.csic.es

Submitted: 19 October 2018 **Approved:** 01 November 2018 **Published:** 04 November 2018

Cite this article: Cespedes A, Perez MJ, Gomara MJ, Wandosell F, Haro I. Atorvastatin in PLGA-PEG Nanoparticles Derivatized with the HIV-TAT Peptide Protects Neuronal Cultures in an Oxygen-Glucose Deprivation (OGD) Model. Am J Nanotechnol Nanomed. 2018; 1(2): 055-063.

ABSTRACT

The development of new nanotechnology-based drug delivery systems, such as Polymer-Based Nanoparticles (NPs), is a new strategy to increase the solubility and bioavailability of many pharmaceutical compounds. Indeed, Poly(Lactic-Co-Glycolic Acid) (PLGA) is one of the most successfully used biodegradable polymers.

The purpose of the current work was to determine whether the neuroprotective efficiency of, Atorvastatin (ATV), was altered when encapsulated using ATV-loaded PLGA NPs. However, the poor aqueous solubility of ATV hinders the in vivo efficacy of this drug. We prepared a biodegradable NP complex based on PLGA with a non-ionic amphiphilic surfactant, Polyethylene Glycol (PEG). We evaluate the biological activity and neuroprotective effects of PLGA-PEG-HIV-TAT/ATV, in comparison with free ATV, using a human neuronal cell line (SH-SY5Y) and primary mouse neuronal cultures as biological models. And next we evaluate the neuroprotective effects of PLGA-PEG-HIV-TAT/ATV, in comparison with free ATV using a cellular model of brain stroke, Oxygen and Glucose Deprivation (OGD).

We first determined toxicity and efficiency of internalization and colocalization within the inner compartments of neuroblastoma cells SH-SY5Y and cortical neurons. The data showed that the NPs could cross the cell membrane, being detected in the cytoplasm as early as 4 h after administration and decreasing through 24 h. NPs did not present toxicity at the concentrations tested, with or without ATV loading. Next, we examined the ability of the PLGA-PEG-HIV-TAT/ATV polymer complex to prevent toxicity and death of SH-SY5Y cells in a model of Oxygen-Glucose Deprivation (OGD) at different concentrations. ATV-loaded NPs, increased cell viability by approximately 85-95% and had no significant cytotoxic effect. The data showed that they could be used as alternative neuroprotective strategy to deliver compounds such as statins. Thus, we propose that these NPs are promising nanosystems for the treatment of some neurological disorders, if they improve the passage of ATV across the blood-brain barrier.

Graphical Abstract:

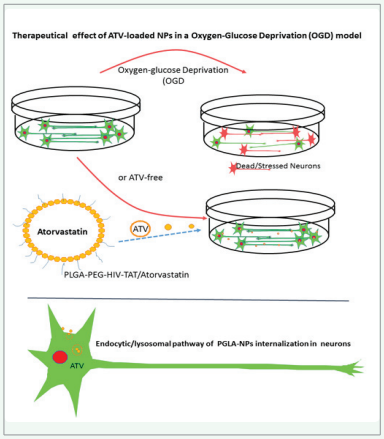

Keywords: Ischemia model; Polymeric nanoparticles; PLGA-PEGylated nanoparticles; HIV-TAT peptide; Atorvastatin

INTRODUCTION

The passage of drugs across cell membranes is perhaps the main obstacle to effective drug administration. In general, administration of drugs at high concentrations are required in order to achieve adequate cellular uptake and the expected effect [1]. The oral route is the most frequent route of drug administration; however, low solubility and absorption of hydrophobic drugs limit the ability to obtain optimal plasma concentrations and most importantly, distribution into target tissues. Recently, the pharmaceutical industry has developed new strategies to increase solubility and bioavailability, among them the development of new nanotechnology-based drug delivery systems, such as Polymer-Based Nanoparticles (NPs) [1]. Following this rationale to increase the bioavailability of unstable hydrophilic drugs such as anthocyanins, polymer-based NPs have been used due to their special characteristics such as high diffusion rate, improved bioavailability and high loading efficiency of water-soluble drugs. Formulations of biodegradable NPs based on Poly(Lactic-Co-Glycolic-Acid) (PLGA) and a Polyethylene Glycol (PEG) stabilizer loaded with anthocyanins have been used for their biological activity and neuroprotective effect [2]. PLGA is one of the most widely used biodegradable polymers because its hydrolysis produces monomers of endogenous metabolites, which are easily eliminated by the body. As PLGA has minimum systemic toxicity for administration of drugs, the United States Federal Drug Administration (FDA) and the European Medicine Agency (EMA) have approved the use of PLGA-based medicines in humans. Alternative NPs such as nano-liposomes, solid lipid NPs, polymeric NPs, polymeric micelles or dendrimers have been proposed [3,4]. The design of PEGylated liposomal forms of doxorubicin has shown substantially increased efficacy in breast cancer treatment [5].

Several statins such as Atorvastatin (ATV), simvastatin, lovastatin, etc., are currently in use to treat hyperlipidemias, reducing cholesterol synthesis through inhibition of 3-hydroxy-3-methylglutaryl-coenzyme A (HMG-CoA) [6]. In addition, it has been described that statins exert beneficial effects in some neurodegenerative diseases, such as Alzheimer's Disease (AD), Multiple Sclerosis (MS), Amyotrophic Lateral Sclerosis (ALS), Parkinson's Disease (PD) and cerebral ischemic stroke. In fact, it is well documented that administration of statins reduces the incidence of primary Cerebrovascular Accident (CVA) and, in the long term, improves neurological functional responses in patients [6]. Among the statins, ATV has low aqueous solubility resulting in low oral bioavailability (12%), and thus presents a challenge to obtain a suitable dosage

form. Solid-phase dispersion techniques have been used to improve the solubility of ATV [7]. It has been reported that lipophilic statins such as simvastatin and lovastatin have the ability to cross the Blood-Brain Barrier (BBB) due to their lipophilic character [6]; however, there are no significant differences in neuroprotection or coronary artery disease between these lipophilic statins and other statins, such as pravastatin and rosuvastatin, which are hydrophilic [8,9]. Thus, the use of NPs may provide a new system of administration of drugs with different solubility properties. Recently, research has focused on the design of solid polymer NPs and lipid systems (liposomes) that confer greater stability and bioavailability to the drug [3].

The efficiency of internalization of NPs through the endothelium depends on the physicochemical characteristics of the particles, in addition to their size. In recent years, significant progress has been made in the field of neuroscience, improving the understanding of the physiopathology of the Central Nervous System (CNS); however, development of successful strategies against major neurological disorders is limited by the protective function of the BBB [10]. It has been reported that NPs have been able to penetrate the BBB and reach the brain 1 h after injection [11-13]. The incorporation of a hydrophilic PEG group on the surface provides resistance to opsonization and phagocytosis, consequently with a longer duration in the blood compared to NPs prepared without PEG [2].

The use of Cell-Penetrating Peptides (CPPs), short amphipathic and cationic peptides that are rapidly internalized across cell membranes, may aid in transport across cell membranes and even the BBB. Generally, they are peptides with chains of less than 30 amino acids (aa) that have the capacity to transport molecules from the extracellular space into the cells [10], and can be used to deliver NPs, molecular cargo such as fluorescent dyes, drugs, liposomes, and peptides [12]. In this way, studies have been carried out with peptides derived from human immunodeficiency virus (HIV-1), Antennapedia (pAntp), the VP22 protein of herpes simplex virus and polyarginine (poly-Arg) sequences, among others [13-15].

The present work is focused on the use of ATV-loaded NPs, analyzing internalization parameters in two neural cell types. The aim of this work was to establish a "proof of concept" of whether ATV presented in NPs is therapeutically more or less neuroprotective than free ATV in a cellular model of brain stroke (oxygen and glucose deprivation; OGD). Our data support the hypothesis that ATV-loaded NPs are as effective as the free compound for recovery from OGD.

MATERIALS AND METHODS

ATV (Atorvastatin®), PLGA (Resomer® RG503H, Poly (D,L-lactide-co-glycolide 50:50), Pluronic® F-68 Polyoxyethylene-polyoxypropylene (Poloxamer), N-diisopropylethylamine (DIEA), ethyl-3-(3-dimethylaminopropyl) carbodiimide hydrochloride (EDC) and NHS (N-Hydroxysuccinimide) were purchased from Sigma-Aldrich (St. Louis, MO, USA). PEG-methyl ether maleimide (Maleimide-PEG-NH2; 2,000 Da) was obtained from Jenkem Technology (Beijing, P.R. China). Acetonitrile was from Fisher Scientific (Loughborough, UK), while diethyl ether, acetone, and methanol were purchased from Merck KGaA (Darmstad, Germany). Dimethylformamide (DMF) was from Scharlau (Barcelona, Spain) and chloroform from Carlo Erba (Cornaredo, MI, Italy).

The HIV-TAT peptide (CGGGGYGRKKRRQRRR) was synthesized by Solid-Phase Peptide Synthesis (SPPS) and characterized by Reversed-Phase High-Performance Liquid Chromatography (RP-HPLC) as described previously [16]. The HIV-TAT peptide contains cationic aa including 6 arginine residues and 2 lysine residues, promoting their uptake by cells and making them more efficient in transport than other cationic homopolymers rich in ornithine and histidine [17,1].

Preparation and characterization of ATV-loaded polymeric NPs

Synthesis and characterization of the polymer PLGA-PEG-HIV-TAT: A combination of 1 g (32.3 µmol) of PLGA (RG 503H), 27 mg (234.6 µmol) of NHS and 45 mg (234.7 µmol) of EDC were dissolved in 2 ml of chloroform in a glass vial. The activation of carboxyl groups of the PLGA took place in the hermetically-sealed vial upon stirring overnight at room temperature. The succinimidyl ester of the PLGA (PLGA-NHS) was precipitated with cold diethyl ether and pelleted by centrifugation, re-dissolved in chloroform and precipitated again with diethyl ether. This process of precipitation/dissolution washing cycle was repeated three times before the activated PLGA-NHS was dried under vacuum, dissolved in chloroform and after adding water, stirring and flash freezing, it was lyophilized.

To obtain the PLGA-PEG-maleimide, 500 mg (16.2 µmol) of PLGA-NHS and 35 mg (17.5 µmol) of maleimide-PEG-NH2 were dissolved in 1 ml of chloroform. The amine reacted with the PLGA-NHS after addition of 20 µl (117.15 µmol) of DIEA with constant stirring overnight in a hermetically-sealed vial. The PLGA-PEG-maleimide was precipitated with cold 80:20 ether:methanol and pelleted by centrifugation, re-dissolved in chloroform and precipitated again with 80:20 ether:methanol. This wash process was repeated three times and the final polymer PLGA-PEG-maleimide was dried under vacuum, dissolved in chloroform and after adding water, stirring and flash freezing, it was lyophilized. Characterization of PLGA-PEG-maleimide was done by proton Nuclear Magnetic Resonance (^{1}H-NMR) after dissolving it in deuterated chloroform. The spectrum was recorded at 298K on a Varian Inova 400 MHz spectrometer (Agilent Technologies, Santa Clara, CA, USA).

Previously, PLGA/PEG NPs loaded with ATV (PLGA-PEG/ATV) were prepared and then to obtain the polymer PLGA-PEG-HIV-TAT, 5 mg (2.6 µmol) of HIV-TAT peptide was dissolved in 500 µl of acetonitrile/DMF (50:50 v/v) and added to a solution of 150 mg (4.0 µmol) PLGA-PEG-maleimide in chloroform. The reaction of the thiol group of the cysteinyl-peptide with the maleimide group of the polymer took place overnight in a sealed vial with stirring. The product was precipitated with cold ether:methanol (50:50, v/v) and pelleted by centrifugation, re-dissolved in chloroform and precipitated again in ether:methanol (50:50, v/v). This wash cycle was repeated twice more before the final PLGA-PEG-peptide was dried under vacuum, dissolved in chloroform and after adding water, stirring and flash freezing, it was lyophilized. Characterization of the PLGA-PEG-HIV-TAT was done by ^{1}H-NMR as described above after dissolving it in deuterated dimethylsulfoxide.

Preparation of ATV-loaded NPs: NPs containing ATV were prepared by the solvent-displacement technique: An organic solution of 45 mg polymer (PLGA-PEG-HIV-TAT or PLGA-PEG) in 2.5 ml of acetone containing 5 mg ATV was poured dropwise with moderate stirring onto 5 ml of an aqueous solution containing 50 mg of Poloxamer (F68). This agent acts as a surfactant and maintains the emulsion depending on the dispersion capacity in water. The NPs were formed instantaneously by rapid diffusion of the solvent

to the aqueous medium. The organic solvent was removed from the suspension by subjecting it to reduced pressure.

Physicochemical characterization of NPs: We used the Nano Zetasizer® Malvern for morphometric determinations (average particle diameter and polydispersity) and surface charge-zeta potential (Z potential) using dynamic light scattering with Non-Invasive Backscatter optics (NIBS), after diluting the NPs 1:10 in milli-Q water. ATV content of the PLGA-PEG-HIV-TAT and PLGA-PEG NPs was quantified by RP-HPLC (1260 Infinity, Agilent Technologies, Santa Clara, CA, USA) in a ZORBAX Eclipse Plus SB-C18 column (100 × 4.6 mm; 3.5 µm) (Agilent Technologies). Isocratic mixture of acetonitrile: water (85:15, v/v), adjusted to pH 4.5 with phosphoric acid, was used as eluent. The analysis was performed at a flow rate of 1 ml/min with a UV detection wavelength of 261 nm. Standard curves were made for quantitation of ATV by plotting RP-HPLC absorption values for different concentrations of the drug.

Transmission Electron Microscopy (TEM) of NPs: Physicochemical characterization was complemented by TEM, using a NPs suspension (100 µl/ml) that had been stirred continuously for 1 h. A drop of NPs (10 µl) was placed in collodion/carbon-coated copper TEM grid (ø 3 mm - 400 mesh), followed by a drop of uranium acetate (2%) that was allowed to air-dry at room temperature and mounted on the microscope scanner. TEM photographs were taken in three or more fields at 3K, 8K, 15K, 25K and 40K, by using the NIH imaged software. (3K = 3000 increases).

Viability assay in SH-SY5Y cells: The putative cytotoxic effects of the ATV solution and ATV-loaded NPs were assayed by the MTT method, as previously described [18-20]. Neuroblastoma cells (SH-SY5Y) were plated at a high density (85% confluent) in 24-well plates (Corning, NY, USA), incubated several hours to permit attachment, and different concentrations of ATV (0.5, 1 and 2 µM), both in solution and NP-loaded, were added to the cell culture medium. The medium was changed on the 2nd day following the drug treatment, and no additional dose of drug was added. Cells treated with only media (1x DMEM) were used as controls, and each test was performed in triplicate. Viability of the cells was determined on the 4th day after drug administration. After the specified incubation time, each well was washed with HBSS to eliminate phenol red and 200 µl (0.5 mg/ml) of MTT was added to each well, and incubated for 1 h at 37°C. The MTT derivative was dissolved in DMSO (500 µL per each well), and the optical density was measured at 550 nm using a microplate reader (Opsys, MR-DINEX Technologies). Differences in viability were expressed as a percentage of absorbance relative to untreated controls [21].

Viability, cytotoxicity and survival of SH-SY5Y cells after treatment with ATV-loaded NPs in an OGD model: Parallel cultures of SH-SY5Y neuronal cells were maintained under optimal CO2 conditions, either at 5% O2 (standard) or in hypoxia chambers (1% O2), with culture medium depleted of glucose, as previously described [21,22]. After 16 h, the cytotoxicity profile was evaluated in SH-SY5Y cells, using the MTT assay [23].

Different cell viability experiments were performed in triplicate, using the OGD model. The first was to establish the effect of ATV alone (0.5, 1.0 and 2.0 µM) on SH-SY5Y cells, under standard incubation conditions (95% CO2 and 5% O2 in DMEM with glucose) *vs.* hypoxic conditions (36% CO2, 63% N2, 1% O2 in DMEM without glucose). The second experiment consisted of determining the effect of ATV in solution and ATV-loaded NPs in SH-SY5Y cells at a single concentration (1.0 µM) in the OGD model *vs.* standard culture conditions.

Cortical primary neuron culture and OGD: Primary mouse neurons were prepared from 17 day-old Swiss mice embryos (E17). A pool of cerebral cortices were dissected and enzymatically digested with 0.05% trypsin-EDTA (Invitrogen) and 10 mg/ml DNase (Roche Applied Science) for 15 min at 37°C, followed by trituration with fire-polished glass pipettes. The cells were plated in 24-well plates for viability experiments and 6-well plates for western blot analysis, at a density of 2.5 x 10^5 cells/ ml. The plates were previously coated with 0.5 mg/ ml poly-L-lysine (Sigma-Aldrich) in borate buffer. Neurons were cultured with Neurobasal Medium (NB) supplemented with 2% B27 and 2 mM glutamine (Invitrogen), and maintained at 37°C in a humidified 95% air/5% CO2 atmosphere incubator. In all experiments, cultures were used after 4 days of maintenance, and contained 90-95% neurons.

For OGD, cultured neurons were incubated in glucose-free DMEM in a near-anaerobic atmosphere containing 1% O2, 5% CO2 and 94% N2 at 37°C. For a control (non-OGD condition) that was considered "normoxic" with respect to standard methods, DMEM media and a normal incubator were used. After 17 h OGD, the cultures were returned to a normal environment; glucose-free media was replaced with NB/B27 media and cultures were returned to a 95% air/5% CO2 incubator. Experimental parameters were assayed 24 h after re-oxygenation/regeneration. Neuronal cultures were treated after OGD with ATV or ATV-loaded NPs as described previous section, for four hours (rescue period).

Immunofluorescence: Immunofluorescence assays were performed as previously described [24,25], with some modifications described below. Fixed neurons were permeabilized in PBS containing 0.25% Triton X-100, followed by incubation with the primary antibody against PEG (PEG-B-47 ab51257; Abcam). In some experiments PEG-positive NPs were localized with respect to early endosome compartment, and lysosomes, using the antibodies against an endosomal marker (Rab5) and a lysosomal marker (CD63), both from Abcam. In some experiments an antibody against tubulin (β-III tubulin, Abcam) was used to label the microtubular network.

After several washes with PBS containing 0.25% Triton X-100, coverslips were incubated with Alexa-555-labeled anti-mouse (1:500; Invitrogen) and with AlexaFluor™ 488 (green) phalloidin (Invitrogen A12379) (1:100) for labeling of F-actin. DAPI (1:5,000) was used to label the nuclei (blue) and confirm cellular integrity.

Statistical analysis: The data are expressed as the mean ± Standard Deviation (SD) of at least three independent experiments. The non-parametric Kruskal-Wallis test followed by the Mann-Whitney U-test was used to investigate significant differences. In all cases, $p < 0.05$ was considered to be statistically significant and $p < 0.001$ highly significant. All data processing was performed using GraphPad® Prism statistical software (7 version).

RESULTS

Physicochemical characterization of PLGA-NPs: TEM and DLS analysis

Three different NP preparations were obtained: PLGA-PEG NPs loaded with ATV (PLGA-PEG/ATV), and PLGA-PEG-HIV-TAT NPs both with (PLGA-PEG-HIV-TAT/ATV) and without (PLGA-PEG-HIV-TAT) drug. The polydispersity index of the three analyzed

samples was low, indicating the formation of almost monodispersed NPs (Figure 1A, B, C). The Z potential of NPs prepared with the PLGA-PEG-HIV-TAT was electropositive, both when loaded with ATV (21.8 ± 0.057 mV) and without drug (23.1 ± 1.2 mV). On the contrary, the Z potential of the ATV-loaded NPs prepared with the PLGA-PEG polymer was electronegative (-20.4 ± 1.02 mV). Thus, the covalent coupling of the HIV-TAT peptide to the PLGA-PEG-maleimide polymer led to a synthetic copolymer that confers cationic charge to the NPs. Simultaneously, the ATV content of the NP preparations was quantified, using RP-HPLC to determine the amount of free drug that was not entrapped in the nanoparticle, after centrifugation and filtration of the samples. The entrapment efficiency was found to be higher than 95%.

Morphological examination by TEM showed NPs with spherical and oval morphology (Figure 2), with an average diameter of 176.4 ± 11.23 nm in the complete assembly (PLGA-PEG-HIV-TAT/ ATV) versus 96.6 ± 1.60 nm in empty NPs (PLGA-PEG-HIV-TAT), whereas PLGA-PEG NPs with ATV (PLGA-PEG/ATV) had a diameter of 158.9 ± 1.37 nm (Figure 2).

Uptake of ATV-loaded NPs by SH-SY5Y cells and primary neurons

Cell uptake analysis was performed to evaluate the ability of human neuroblastoma SH-SY5Y cells and cortical neurons to engulf NPs. In order to investigate intracellular retention, ATV-loaded NPs were diluted in DMEM or in NB/B27 for addition to SH-SY5Y cells or primary neurons, respectively. After incubation for 2, 4, 8, 16 or 24 h, cells were fixed and stained with anti-PEG antibodies, and phalloidin to show F-Actin of the cytoskeleton. The images show that ATV-loaded NPs were effectively absorbed and internalized by SH-SY5Y cells (Figure 3A) and cortical neurons (Figure 3B), as early as 2 h after administration. The data showed that a maximum of PEG-positive signal was reached after 4 h incubation, with decreasing levels thereafter in SH-SY5Y (Figure 3A) and cortical neurons (Figure 3B), being clearly lower after 24 h. Cellular localization with respect to the nuclei (DAPI-stained) indicated perinuclear distribution with a vesicular-like structure (Figure 3C).

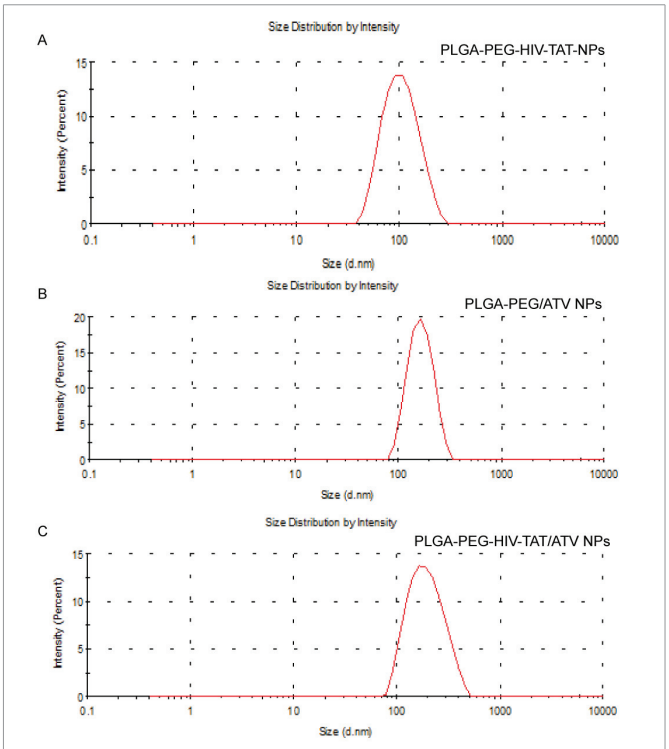

Figure 1: Dynamic Light Scattering (DLS) determination. We determined the particle size (nm), electrokinetic potential (potential of mV) and polydispersity index of the assembly of three nanosuspensions: A) PLGA-PEG HIV-TAT; B) PLGA-PEG/ATV; and C) PLGA-PEG-HIV-TAT/ATV

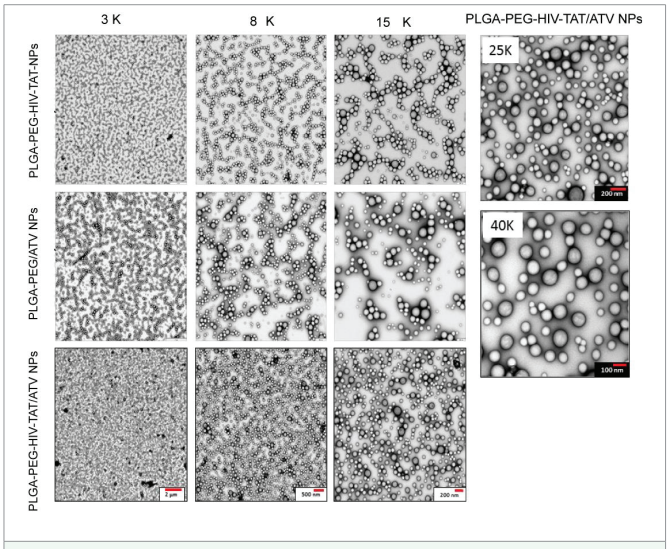

Figure 2: Transmission electron micrographs of different assembled NPs. Three different microphotographs for each nanosuspension (PLGA-PEG-HIV-TAT, PLGA-PEG/ATV and PLGA-PEG-HIV-TAT/ATV, respectively from top to bottom) were obtained at three different magnifications (3K, 8K, and 15K). Scale bars (red line) were used to specify length in micrographs at each magnification (2 µm, 500 nm and 200 nm, respectively). In all cases, spherical morphology and particles size was observed to confirm DLS measurements. Two higher magnification (25K and 40K) images of PLGA-PEG-HIV-TAT/ ATV are presented in the right panel (K = 1000x).

To further define these NPs, several antibodies were used against specific proteins that mostly localize in endosomes, Golgi or lysosomes. Confocal microscopy showed that ATV-loaded NPs colocalized with the early endosome marker Rab5 (12.67%) (Figure 3C), and also with the lysosomal marker CD63 (58%), strongly suggesting that the NPs enter the cell through an endosomal-lysosomal pathway.

ATV-loaded NPs improved SH-SY5Y and neuronal survival after OGD

An important aim of our work was to identify whether ATV administration via NPs is as effective as ATV applied in solution. First, ATV in solution was tested for cytotoxicity and its capacity to recover a cellular model of OGD. ATV in solution (0.5, 1.0 and 2.0 µM) was incubated with cells for 18 h, and cell survival was tested by the MTT assay. There was a decrease in cell viability and slightly harmful effect of 2 µM ATV with respect to the controls, under standard incubation conditions (Figure 4A). To determine whether ATV in solution could enhance cell recovery after OGD, it was added to the cell culture medium at different concentrations, resulting in an increase in cell viability (Figure 4A).

In parallel experiments, we determined that ATV-loaded NPs did not possess any significant cytotoxic effects, with 85-95% cell viability observed by the MTT method. Next we compared ATV in solution (1 µM) and ATV-loaded NPs in a model of OGD in SH-SY5Y cells. Under standard culture conditions (normoxia), no changes in

viability were observed in either treated groups when compared with controls (Figure 4B). After OGD, there was a clear reduction in viable cells that was prevented by the presence of either ATV solution or ATV-loaded NPs (Figure 4B).

Next, these observations were extended to primary neurons. In conditions of normoxia, the ATV-loaded NPs increased cell viability, as determined by MTT, and after OGD both the ATV solution and the ATV-loaded NPs increased cell viability, with highly significant differences from the untreated control group ($p < 0.0001$)(Figure 5A).

To confirm that ATV and ATV-loaded NPs improved neuronal viability, we used the microtubule network as a reference of neuronal integrity. Thus in parallel cultures, neurons treated and untreated with NPs, were fixed and stained with antibodies against β-tubulin, showing that the Microtubular Network (MT) was modified after OGD, taking on a more punctuate aspect. In contrast, a linear MT aspect was clearly recovered after OGD in cells treated with ATV solution or ATV-loaded NPs (Figure 5B), suggesting that effect of ATV was indistinguishable between methods of drug delivery.

DISCUSSION

Nanomedicine, the medical application of nanotechnology, promises a limitless range of applications from biomedical imaging to drug delivery and therapeutics [26]. Nanotechnology is a rapidly-developing field with great potential for research and applications in

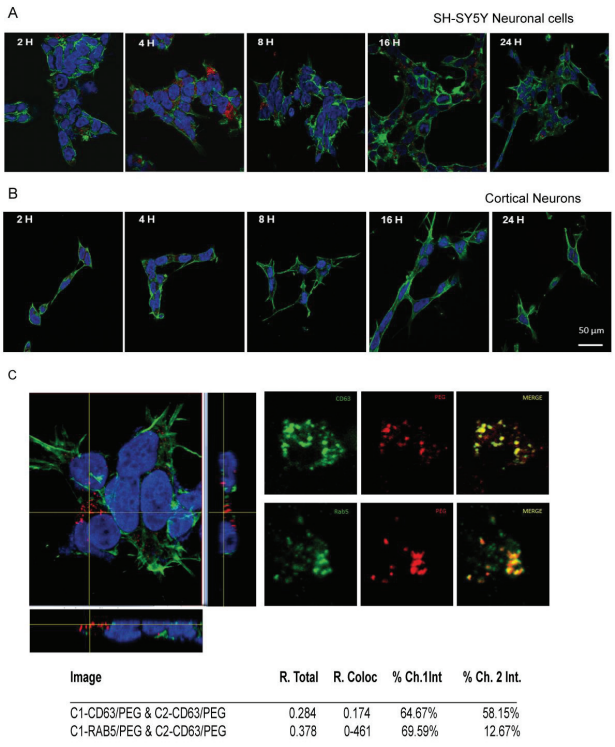

Figure 3: Confocal laser scanning fluorescence images showing the uptake of PLGA-PEG-HIV-TAT/ATV. The IFs represent a time-course of NPs incorporation within SH-SY5Y cells (A), or cortical neurons (B). Cell were fixed at different time points (from 2-24 h) and stained with anti-PEG polyclonal antibody (red), and F-actin was observed using phalloidin (green); the microphotographs were taken at 63x. C) In a parallel experiment, the percentage of colocalization was determined between PEG-positive NPs and the early endosome marker Rab5 (12.67%) and the lysosomal marker CD63 (58%).

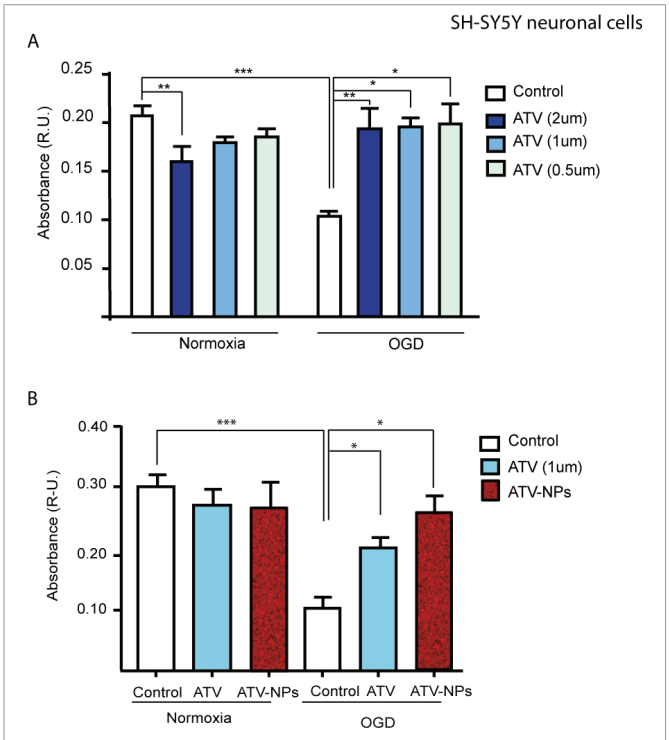

Figure 4: Effects of different Atorvastatin (ATV) concentrations on viability of SH-SY5Y cells. (A) Different concentrations of ATV in solution were assayed in normal growth conditions (normoxia), or in a model of Oxygen and Glucose Deprivation (OGD), as described in the Materials and Methods. (B) In parallel experiments, a single concentration of ATV in solution was compared with NPs loaded with similar amounts of ATV in normoxia or in a model of OGD. Differences in viability were determined by MTT assay, and the data plotted as the mean ± SD of three separate experiments. Cut offs for statistical significance were established at $p < 0.05$ (*), $p < 0.005$ (**) and $p < 0.001$ (***).

the prevention and treatment of various pathologies associated with human diseases. Nanoparticles based on biodegradable and relatively innocuous polymers, such as PLGA-PEG, have been widely researched as drug delivery systems that are encapsulated and protected from antigen recognition, opsonization and tissue degradation, allowing for controlled release and improved distribution to target tissues. In addition, PLGA and PEG are approved by the USFDA and EMA for employment in various drug delivery systems, both in preclinical and clinical studies. The aim of the current work was to prepare and characterize a series of derivative NPs containing a representative drug, ATV. The purpose was to determine if this drug incorporated within NPs was more or less effective than the original drug alone, in recovery from OGD *in vitro*.

In this study, we prepared PLGA-PEG-HIV-TAT NPs loaded with ATV, and completely characterized them from a physicochemical perspective (particle size, polydispersity, Z potential, encapsulation efficiency, morphology, etc.). For the present work we did not compare NPs with TAT and without TAT. We have assumed that the presence of TAT facilitates entry into neuronal or non-neuronal cells [27,28]. Similarly, we assume that the presence of PEG help to NPs evade from clearence mechanisms present in the systemic circulation and the body [29]. The NPs varied in size depending on the addition of ATV, though all fell into an acceptable nanometric range (96-176 nm), and had a positive Z potential of 23.1 ± 1.2 mV (empty NP) and 21.2 ± 0.057 mV (ATV-loaded). Polydispersity, a measure of the heterogeneity of particle sizes in the mixture, was very low (0.122 ±

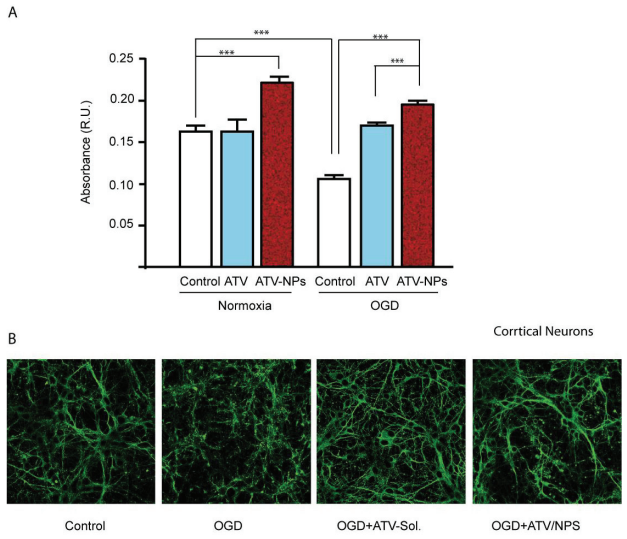

Figure 5: Effects of different Atorvastatin (ATV) concentrations on viability of primary cortical neurons. The effects of similar concentrations of ATV and ATV-loaded NPs were compared in primary cortical neurons, growing in standard conditions (normoxia), and in a model of Oxygen and Glucose Deprivation (OGD), as described in the Materials and Methods. (A) Differences in viability were determined by MTT assay, and the data plotted as the mean ± SD of three separate experiments. Cutoffs for statistical significance were established at $p < 0.05$ (*), $p < 0.005$ (**) and $p < 0.001$ (***). (B) In parallel cultures, cortical neurons subjected to OGD were incubated with ATV in solution, ATV-loaded NPs, or control media (OGD). After four hours neurons were fixed and stained with anti-tubulin, with untreated neurons serving as a reference for the Microtubular network (MT) (Control).

0.004 and 0.149 ± 0.023, respectively for empty NPs and ATV-loaded NPs). Additionally, the efficiency of encapsulation of ATV was greater than 95%, which permitted subsequent comparative analyses to the unbound drug.

A major obstacle to the delivery of peptide and protein medications is their limited bioavailability, inadequate stability, immunogenicity, and limited permeability across biological membranes. However, nanotechnology can increase the uptake of these peptides by cells [26,30]. In particular, the effective transport of anti-viral peptides through the vaginal epithelium by means of PLGA NPs coated with glycol-chitosan has been recently demonstrated [30,31]. Furthermore, several small regions within proteins, called Protein Transduction Domains (PTDs) or Cell-Penetrating Peptides (CPPs) can be used to permit delivery of exogenous substances into living cells [31,32]. In the present study, a small peptide of 16 aa (HIV-TAT) has been used to improve the delivery of ATV from PLGA-PEG NPs across neuronal cell membranes. It is likely that HIV-TAT promotes diffusion of ATV encapsulated in the PLGA-PEG NPs across the membrane, acting as a CPP nanovehicle, as recently reported to transport of other drugs through a lipid membrane [26].

Similarly, in other studies, DNA transfection *in vivo* has been improved using liposomes modified with HIV-TAT-like peptides, coated with PEG to protect the peptide from nonspecific interactions between the liposome and the cell [17]. Recently was reported that Chitosan-PEG-TAT polymer could deliver a functional siRNA against the Ataxin-1, supporting that idea that NPs modify with PEG and TAT would be an useful tool in neurodegenerative pathologies [32].

TEM analysis showed at the highest magnification (8K and 15K) that NPs presented predominantly spherical shapes. It has been commonly assumed that the outer region corresponds to the hydrophilic PEG segment, with an internal hydrophobic amorphous core similar to that reported by Li and others [31]. The negative Z potential has been considered by other authors [2,33] as an important indicator of stability of similar dispersions. The negatively charged NPs provides extra stability due the putative repulsion among NPs. In addition, it has been proposed that the anionic charge of NPs would allow better cross the BBB, compared to cationic NPs. In future experiments, this aspect must be further evaluated.

Before studying the NPs *in vitro*, cytotoxic effects of the ATV at different concentrations were determined. A dose of 2 μM ATV in solution was found to be the highest concentration suitable for using in our neuronal neuroblastoma cell line (SH-SY5Y). There was no apparent toxicity in SH-SY5Y or in primary neurons when we used PLGA-PEG-HIV-TAT/ATV nanoparticles in concentration nearby to 1 μm of free ATV.

Next we evaluated the cellular uptake, diffusion, residence time and putative route of internalization recently, the mechanism of uptake of CPPs has become very controversial, due in many cases to a lack of knowledge about the active conformational structure of peptides and polymeric complexes at the time of penetration and translocation across the membrane [14].

The time course study of NP uptake in SH-SY5Y cells showed internalization as early as 2 h after treatment, remaining detectable through 24 h, although at significantly lower levels. The fact that detected NPs steadily decreased from a peak at 4 h after treatment over time is consistent with activation of cellular metabolism for their elimination, without presenting cellular toxicity. Indeed, viability in NP-treated cells was very similar to that of the untreated control groups.

The presence of the intracellular PEG-positive signal corresponds to the entry of ATV-loaded NPs, this internalization may correspond with either endocytosis or transcytosis [10]. In fact, endocytosis and direct penetration of molecular cargo have been suggested as the two major uptake mechanisms, which is still under debate [35]. We think that the endocytic pathway is involved in the transport of NPs. Our data indicated a clear colocalization PEG positive signals with Rab5 (12.67%), an early endosome marker [34], and CD63 (58.14%) which participates in the lysosomal pathway 4 hours after NPs delivery. Rab5 belongs to the Ras small GTPase superfamily, as does Rab7. Membrane trafficking from the early endosome to the late endosome is determined by the recruitment of Rab5 to early endosomes and, sequentially, acquisition of Rab7 followed by loss of Rab5 in the late endosomes [34]. On the other hand, colocalization of CD63 with the NPs suggests that a significant fraction of NPs that enter the cells follow the lysosomal route. This strongly support that PLGA-PEG-HIV-TAT/ATV is internalized using the endosomal-lysosomal pathway. As described in other studies [35,36], the simple cytosolic persistence of the NPs stained with anti-PEG did not affect the cyto-architecture of the SH-SY5Y cells. In our study, cell morphology and viability were similar to the controls in both normoxia and OGD.

The *in vitro* release of anthocyanin nanoparticles and resveratrol has been previously demonstrated, exhibiting a biphasic kinetic including rapid drug diffusion, followed by a continued release dependent on the characteristics of the particular drug. It is tantalizing to hypothesize that ATV may be liberated from PLGA-PEG-HIV-TAT NPs by a similar route, generating a therapeutic

effect [37,38]. In fact it has been reported that ATV may improve a murine model of Middle Cerebral Artery Occlusion (MCAO), when administered after brain damage [39]. Thus, as a "proof of concept" we compared the neuroprotective efficacy of free ATV with its NP-entrapped counterpart. A cellular model of primary cortical neurons were depleted glucose and oxygen for a specific time period, to mimic a brain stroke [40,41]. Both forms of ATV administration obtained a similar neuroprotective response, confirming that NPs loaded with ATV is an excellent mode of drug delivery. We must assume that ATV in the endosomal/lysosomal system is released from NPs, and exert its therapeutic action, in a similar way as it makes it free. However, it remains to be established whether in animal models of MCAO the efficiency of these CPPs will be similar to cell culture. Obviously, the complexity of multiple cellular systems must be considered *in vivo*, and the CPP are dispersed throughout nearly the entire body, independently of the route of administration (oral, intravenous or intraperitoneal).

Cellular association and trafficking of NPs enables us to understand both the context-dependent phenomena in various disease states, and the potential therapeutic approaches [42,45]. Still, the challenge is to formulate a combination of encapsulated agent with a targeted drug delivery, which will ensure the medicine reaches its target site effectively.

Both *in vitro* and *in vivo* assays, CPPs have proven to be valuable tools for transport across the cell membrane, including nanoparticulate pharmaceutical carriers (e.g., liposomes, micelles) [43]. For instance, Matrix Metalloproteinase (MMPs), particularly gelatinases (MMP-2/-9), are involved in neurovascular deterioration after stroke, so the *in vivo* detection can provide information on the disruption of BBB. In a recent report, the authors used cell penetration peptides that activated gelatinase, allowing to establish its activity in primary neuronal cultures and even in the brain of ischemic mice [44]. In addition, several CPPs have been investigated in models of ischemia reperfusion in rats, demonstrating a significant reduction in infarct volumes and neurological deficit after the MCAO [45]. Similar to what happens with the activation of CPPs by gelatinase action after cerebral infarction [46] it is possible that the HIV-TAT peptide coupled to the NPs is able to reach neurons by the disruption of the BBB and promotes diffusion of the ATV encapsulated inside the neurons.

In summary, encapsulation in PLGA-PEG-HIV-TAT NPs provides an excellent mechanism to deliver specific compounds to neurons. As a proof of concept, our data showed that those NPs containing neuroprotective compounds could be used as an alternative drug supply system to free delivery of pharmacological agents, such as statins. Our data strongly suggest that PLGA-NPs are internalized using a endocytic/lysosomal pathway. We demonstrate that in a cellular OGD model, ATV-loaded NPs-administration is as good as free ATV, perhaps with even lower toxicity. With all these data it is tantalizing to propose that similar NPs improved to cross BBB, may be promising systems for the treatment of some neurological disorders.

ACKNOWLEDGEMENTS

We are grateful to all members of I.H Lab at the Unit of Synthesis and Biomedical Applications of IQAC-CSIC, and the FW Lab in the Centro de Biología Molecular "Severo Ochoa" (CBM SO) for thoughtful discussions during the preparation of this manuscript. The authors gratefully acknowledge the technical assistance and advice of Confocal Microscopy Service at the CBMSO. The professional editing service NB Revisions was used for technical editing of the manuscript prior to submission.

Grants

I.H was supported from the Spanish Ministry of Economy, Industry and Competitiveness (MINECO) and the European Regional Development Fund (Grant CTQ2015-63919-R). F.W was supported by grants from the MINECO/FEDER SAF2015-70368-R, CAM (B2017/BMD-3700), Centro de Investigación Biomédica en Red sobre Enfermedades Neurodegenerativas (CIBERNED); "Proyectos Colaborativos" (PI2016/01) CIBERNED; and by an institutional grant from the Fundación Ramón Areces to CBMSO and Fondos FEDER. In addition, A.C. was supported by a postdoctoral contract from the program: "FORMACIÓN DE TALENTO HUMANO DE ALTO NIVEL.", from Universidad del Tolima; Ibagué-Colombia.

REFERENCES

1. Amsa P, Tamizharasi S, Jagadeeswaran M, Sivakumar T. Preparation and solid state characterization of simvastatin nanosuspensions for enhanced solubility and dissolution. International Journal of Pharmacy and Pharmaceutical Sciences. 2014; 6: 265-269. https://goo.gl/tr8m3a

2. Amin FU, Shah SA, Badshah H, Khan M, Kim MO. Anthocyanins encapsulated by PLGA@PEG nanoparticles potentially improved its free radical scavenging capabilities via p38/JNK pathway against Abeta1-42-induced oxidative stress. J Nanobiotechnology. 2017; 15: 12. https://goo.gl/LtT11c

3. Dilnawaz F, Singh A, Mewar S, Sharma U, Jagannathan NR, Sahoo SK. The transport of non-surfactant based paclitaxel loaded magnetic nanoparticles across the blood brain barrier in a rat model. Biomaterials. 2012; 33: 2936-2951. https://goo.gl/nPL3Lq

4. Masserini M. Nanoparticles for brain drug delivery. ISRN Biochem. 2013; 2013: 238428. https://goo.gl/mbiqBX

5. Tiwari G, Tiwari R, Sriwastawa B, Bhati L, Pandey S, Pandey P, et al. Drug delivery systems: an updated review. Int J Pharm Investig. 2012; 2: 2-11. https://goo.gl/kcyGn8

6. Saeedi Saravi, Saeedi Saravi, Arefidoust A, Dehpour AR. The beneficial effects of HMG-CoA reductase inhibitors in the processes of neurodegeneration. Metab Brain Dis. 2017; 32: 949-965. https://goo.gl/4Tn2jg

7. Ankush Choudhary, Avtar C. Ranaa, Geeta Aggarwal, Virender Kumar, Foziyah Zakir. Development and characterization of an atorvastatin solid dispersion formulation using skimmed milk for improved oral bioavailability. Acta Pharmaceutica Sinica B. 2012; 2: 421-428. https://goo.gl/8DsH7U

8. Bytyçi I, Bajraktari G, Bhatt DL, Morgan CJ, Ahmed A, Aronow WS, et al. Hydrophilic *vs* lipophilic statins in coronary artery disease: a meta-analysis of randomized controlled trials. J Clin Lipidol. 2017; 11: 624-637. https://goo.gl/UchJuc

9. Wood WG, Eckert GP, Igbavboa U, Muller WE. Statins and neuroprotection: a prescription to move the field forward. Ann N Y Acad Sci. 2010; 1199: 69-76. https://goo.gl/y8ADLs

10. Sharma G, Lakkadwala S, Modgil A, Singh J. The role of cell-penetrating peptide and transferrin on enhanced delivery of drug to brain. Int J Mol Sci, 2016. 17: 806. https://goo.gl/rbzrem

11. Simşek S, Eroglu H, Kurum B, Ulubayram K. Brain targeting of Atorvastatin loaded amphiphilic PLGA-b-PEG nanoparticles. J Microencapsul. 2013; 30: 10-20. https://goo.gl/sEmbZa

12. Bolhassani A. Potential efficacy of cell-penetrating peptides for nucleic acid and drug delivery in cancer. Biochim Biophys Acta. 2011; 1816: 232-246. https://goo.gl/vP8opc

13. Lewin M, Carlesso N, Tung CH, Tang XW, Cory D, Scadden DT, et al.

Tat peptide-derivatized magnetic nanoparticles allow in vivo tracking and recovery of progenitor cells. Nat Biotechnol. 2000; 18: 410-414. https://goo.gl/z96Mdy

14. Sebastien Deshayes, Annie Heitz, May C. Morris, Pierre Charnet, Gilles Divita, Frederic Heitz. Insight into the mechanism of internalization of the cell-penetrating carrier peptide Pep-1 through conformational analysis. Biochemistry. 2004; 43: 1449-1457. https://goo.gl/5A5fLW

15. Egleton RD, TP Davis. Development of neuropeptide drugs that cross the blood-brain barrier. NeuroRx. 2005; 2: 44-53. https://goo.gl/4vgKtC

16. Vasconcelos A, Vega E, Perez Y, Gomara MJ, Garcia ML, Haro I. Conjugation of cell-penetrating peptides with poly(lactic-co-glycolic acid)-polyethylene glycol nanoparticles improves ocular drug delivery. Int J Nanomedicine. 2015; 10: 609-631. https://goo.gl/W4dM9s

17. Vives E, J Schmidt, Pelegrin A. Cell-penetrating and cell-targeting peptides in drug delivery. Biochim Biophys Acta. 2008; 1786: 126-138. https://goo.gl/evCyq2

18. Xu MF, Xiong YY, Liu JK, Qian JJ, Zhu L, Gao J. Asiatic acid, a pentacyclic triterpene in Centella asiatica, attenuates glutamate-induced cognitive deficits in mice and apoptosis in SH-SY5Y cells. Acta Pharmacol Sin. 2012; 33: 578-587. https://goo.gl/72Mpxt

19. Abe K, N Matsuki. Measurement of cellular 3-(4,5-dimethylthiazol-2-yl)-2,5-diphenyltetrazolium bromide (MTT) reduction activity and lactate dehydrogenase release using MTT. Neurosci Res. 2000; 38: 325-329. https://goo.gl/NgpY3m

20. Cheung YT, Lau WK, Yu MS, Lai CS, Yeung SC, So KF, Chang RC, et al. Effects of all-trans-retinoic acid on human SH-SY5Y neuroblastoma as *in vitro* model in neurotoxicity research. Neurotoxicology. 2009; 30: 127-135. https://goo.gl/6EEmZj

21. Tabakman R, Jiang H, Shahar I, Arien-Zakay H, Levine RA, Lazarovici P. Neuroprotection by NGF in the PC12 in vitro OGD model: involvement of mitogen-activated protein kinases and gene expression. Ann N Y Acad Sci. 2005; 1053: 84-96. https://goo.gl/jEABRo

22. Wang S, Xing Z, Vosler PS, Yin H, Li W, Zhang F, et al. Cellular NAD replenishment confers marked neuroprotection against ischemic cell death: role of enhanced DNA repair. Stroke. 2008; 39: 2587-2595. https://goo.gl/SkFZn6

23. Lewinski N, V Colvin, R Drezek. Cytotoxicity of nanoparticles. Small. 2008; 4: 26-49. https://goo.gl/jctxiN

24. Baggett JJ, Shaw JD, Sciambi CJ, Watson HA, Wendland B. Fluorescent labeling of yeast. Curr Protoc Cell Biol. 2003; 13. https://goo.gl/ZkGpLa

25. Mao SY, Mullins JM. Mullins, Conjugation of fluorochromes to antibodies. Methods Mol Biol. 2010; 588: 43-48. https://goo.gl/84zCwk

26. Bawarski WE, Chidlowsky E, Bharali DJ, Mousa SA. Emerging nanopharmaceuticals. Nanomedicine. 2008; 4: 273-282. https://goo.gl/EHDr7d

27. Malhotra M, Tomaro-Duchesneau C, Saha S, Kahouli I, Prakash S. Development and characterization of chitosan-PEG-TAT nanoparticles for the intracellular delivery of siRNA. Int J Nanomedicine. 2013; 8: 2041-2052. https://goo.gl/hqSk34

28. Wen X, Wang K, Zhao Z, Zhang Y, Sun T, Zhang F, et al. Brain-targeted delivery of trans-activating transcriptor-conjugated magnetic PLGA/lipid nanoparticles. PLoS One. 2014; 9: 106652. https://goo.gl/TvbuWA

29. Rafiei P, A Haddadi. Docetaxel-loaded PLGA and PLGA-PEG nanoparticles for intravenous application: pharmacokinetics and biodistribution profile. Int J Nanomedicine. 2017; 12: 935-947. https://goo.gl/Q86qcg

30. Ariza Saenz M, Espina M, Bolanos N, Calpena AC, Gomara MJ, Haro I, et al. Penetration of polymeric nanoparticles loaded with an HIV-1 inhibitor peptide derived from GB virus C in a vaginal mucosa model. Eur J Pharm Biopharm. 2017; 120: 98-106. https://goo.gl/7CEwkJ

31. Li X, Li R, Qian X, Ding Y, Tu Y, Guo R, et al. Superior antitumor efficiency of cisplatin-loaded nanoparticles by intratumoral delivery with decreased tumor metabolism rate. Eur J Pharm Biopharm. 2008; 70: 726-734. https://goo.gl/43eGVs

32. Malhotra M, Tomaro Duchesneau C, Prakash S. Synthesis of TAT peptide-tagged PEGylated chitosan nanoparticles for siRNA delivery targeting neurodegenerative diseases. Biomaterials. 2013; 34: 1270-1280. https://goo.gl/g693Sh

33. Lockman PR, Koziara JM, Mumper RJ, Allen DD. Nanoparticle surface charges alter blood-brain barrier integrity and permeability. J Drug Target. 2004; 12: 635-641. https://goo.gl/Aw5hwr

34. Lockman PR, Koziara JM, Mumper RJ, Allen DD. Rab7: roles in membrane trafficking and disease. Biosci Rep. 2009; 29: 193-209. https://goo.gl/3fZhae

35. Bi C, Wang A, Chu Y, Liu S, Mu H, Liu W, et al. Intranasal delivery of rotigotine to the brain with lactoferrin-modified PEG-PLGA nanoparticles for Parkinson's disease treatment. Int J Nanomedicine. 2016; 11: 6547-6559. https://goo.gl/txaQBj

36. Guan Q, Sun S, Li X, Lv S, Xu T, Sun J, et al. Preparation, *in vitro* and *in vivo* evaluation of mPEG-PLGA nanoparticles co-loaded with syringopicroside and hydroxytyrosol. J Mater Sci Mater Med. 2016; 27: 24. https://goo.gl/xuWNKi

37. Chiste RC, Lopes AS, G.De Faria LJ. Thermal and light degradation kinetics of anthocyanin extracts from mangosteen peel (*Garcinia mangostana* L.) International Journal of Food Science and Technology. 2010; 45: 902-908. https://goo.gl/nGZRaL

38. Cevallos-Casals BA, Cisneros-Zevallos L. Stoichiometric and kinetic studies of phenolic antioxidants from Andean purple corn and red-fleshed sweetpotato. J Agric Food Chem. 2003; 51: 3313-3319. https://goo.gl/ioyk3u

39. Amarenco P, Moskowitz MA. The dynamics of statins: from event prevention to neuroprotection. Stroke. 2006; 37: 294-296.

40. Zhou X, Wang Z, Huang W, Lei QY. Protein-coupled receptors: bridging the gap from the extracellular signals to the Hippo pathway. Acta Biochim Biophys Sin (Shanghai). 2015; 47: 10-15. https://goo.gl/dqwRHd

41. Baldassarro VA, Marchesini A, Facchinetti F, Villetti G, Calza L, Giardino L. Cell death in pure-neuronal and neuron-astrocyte mixed primary culture subjected to oxygen-glucose deprivation: The contribution of poly(ADP-ribose) polymerases and caspases. Microchemical Journal. 2018; 36: 215-222. https://goo.gl/YuaACh

42. Behzadi S, Serpooshan V, Tao W, Hamaly MA, Alkawareek MY, Dreaden EC, et al. Cellular uptake of nanoparticles: journey inside the cell. Chem Soc Rev. 2017; 46: 4218-4244. https://goo.gl/NvqPpc

43. Kang T, Gao X, Chen J. Harnessing the capacity of cell-penetrating peptides for drug delivery to the central nervous system. Curr Pharm Biotechnol. 2014; 15: 220-230. https://goo.gl/br6FQn

44. Chen S, Cui J, Jiang T, Olson ES, Cai QY, Yang M, et al. Gelatinase activity imaged by activatable cell-penetrating peptides in cell-based and in vivo models of stroke. J Cereb Blood Flow Metab. 2017; 37: 188-200. https://goo.gl/Q9PV5b

45. Guidotti G, Brambilla L, Rossi D. Cell-penetrating peptides: from basic research to clinics. Trends Pharmacol Sci. 2017; 38: 406-424. https://goo.gl/966Bhn

46. Zhang F, Wang S, Signore AP, Chen J. Neuroprotective effects of leptin against ischemic injury induced by oxygen-glucose deprivation and transient cerebral ischemia. Stroke. 2007; 38: 2329-2336. https://goo.gl/txBxR8